# Gene transcription ontogeny of hypothalamic-pituitary-thyroid axis development in early-life stage fathead minnow and zebrafish

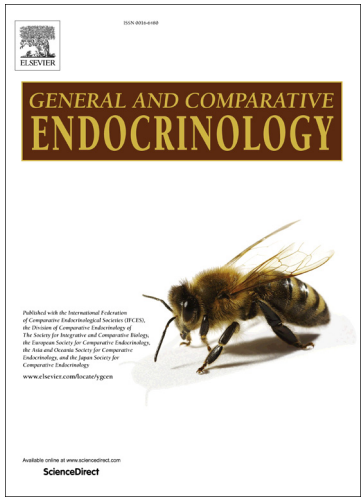


# Gene transcription ontogeny of hypothalamic-pituitary-thyroid axis development in early-life stage fathead minnow and zebrafish

Lucia Vergauwen, Jenna E. Cavallin, Gerald T. Ankley, Chloé Bars, Isabelle J. Gabriëls, Ellen D.G. Michiels, Krysta R. Fitzpatrick, Jelena Periz-Stanacev, Eric C. Randolph, Serina L. Robinson, Travis W. Saari, Anthony L. Schroeder, Evelyn Stinckens, Joe Swintek, Steven J. Van Cruchten, Evy Verbueken, Daniel L. Villeneuve, Dries Knapen

PII: S0016-6480(18)30039-X
DOI: https://doi.org/10.1016/j.ygcen.2018.05.001
Reference: YGCEN 12927

To appear in: *General and Comparative Endocrinology*

Received Date: 12 January 2018
Revised Date: 23 March 2018
Accepted Date: 3 May 2018

Please cite this article as: Vergauwen, L., Cavallin, J.E., Ankley, G.T., Bars, C., Gabriëls, I.J., Michiels, E.D.G., Fitzpatrick, K.R., Periz-Stanacev, J., Randolph, E.C., Robinson, S.L., Saari, T.W., Schroeder, A.L., Stinckens, E., Swintek, J., Van Cruchten, S.J., Verbueken, E., Villeneuve, D.L., Knapen, D., Gene transcription ontogeny of hypothalamic-pituitary-thyroid axis development in early-life stage fathead minnow and zebrafish, *General and Comparative Endocrinology* (2018), doi: https://doi.org/10.1016/j.ygcen.2018.05.001

# Gene transcription ontogeny of hypothalamic-pituitary-thyroid axis development in early-life stage fathead minnow and zebrafish

Lucia Vergauwen[a,b,$], Jenna E. Cavallin[c,$], Gerald T. Ankley[d], Chloé Bars[e], Isabelle J. Gabriëls[a], Ellen D.G. Michiels[a], Krysta R. Fitzpatrick[d], Jelena Periz-Stanacev[a], Eric C. Randolph[f], Serina L. Robinson[g], Travis W. Saari[d], Anthony L. Schroeder[h], Evelyn Stinckens[a], Joe Swintek[c], Steven J. Van Cruchten[e], Evy Verbueken[e], Daniel L. Villeneuve[d], Dries Knapen[a]

[a] University of Antwerp, Zebrafishlab, Veterinary Physiology and Biochemistry, Dept. Veterinary Sciences, Universiteitsplein 1, 2610 Wilrijk, Belgium

[b] University of Antwerp, Systemic Physiological and Ecotoxicological Research (SPHERE), Dept. Biology, Groenenborgerlaan 171, 2020 Antwerp, Belgium

[c] Badger Technical Services, US EPA, Mid-Continent Ecology Division, 6201 Congdon Blvd., Duluth, MN 55804, USA

[d] US EPA, Mid-Continent Ecology Division, 6201 Congdon Blvd., Duluth, MN 55804, USA

[e] University of Antwerp, Applied Veterinary Morphology, Dept. Veterinary Sciences, Universiteitsplein 1, 2610 Wilrijk, Belgium

[f] ORISE Research Participation Program, US EPA Mid-Continent Ecology Division, 6201 Congdon Blvd., Duluth, MN 55804, USA

[g] St. Olaf College, 1520 St. Olaf Ave., Northfield, MN 55057, USA

[h] University of Minnesota-Crookston, Math, Science, and Technology Department, 2900 University Ave., Crookston, MN 56716, USA

[$] Equally contributed

* Corresponding author:

Lucia Vergauwen (Lucia.Vergauwen@uantwerpen.be)

Campus Drie Eiken

Universiteitsplein 1

2610 Wilrijk Belgium

Jenna E. Cavallin (Cavallin.Jenna@epa.gov)

Gerald T. Ankley (Ankley.Gerald@epa.gov)

Chloé Bars (Chloe.Bars@uantwerpen.be)

Isabelle J. Gabriëls (Isabelle.Gabriels@uantwerpen.be)

Ellen D.G. Michiels (Ellen.Michiels@uantwerpen.be)

Krysta R. Fitzpatrick (nels6888@d.umn.edu)

Jelena Periz-Stanacev (Jelena.PerizStanacev@uantwerpen.be)

Eric C. Randolph (ecr77@rsmas.miami.edu)

Serina L. Robinson (robi0916@umn.edu)

Travis W. Saari (tsaari987@gmail.com)

Anthony L. Schroeder (aschroed@crk.umn.edu)

Evelyn Stinckens (Evelyn.Stinckens@uantwerpen.be)

Joe Swintek (swintek.joe@epa.gov)

Steven J. Van Cruchten (Steven.VanCruchten@uantwerpen.be)

Evy Verbueken (Evy.Verbueken@uantwerpen.be)

Daniel L. Villeneuve (Villeneuve.Dan@epa.gov)

Dries Knapen (Dries.Knapen@uantwerpen.be)

**Abstract**

The hypothalamic-pituitary-thyroid (HPT) axis is known to play a crucial role in the development of teleost fish. However, knowledge of endogenous transcription profiles of thyroid-related genes in developing teleosts remains fragmented. We selected two model teleost species, the fathead minnow (*Pimephales promelas*) and the zebrafish (*Danio rerio*), to compare the gene transcription ontogeny of the HPT axis. Control organisms were sampled at several time points during embryonic and larval development until 33 days post-fertilization. Total RNA was extracted from pooled, whole fish, and thyroid-related mRNA expression was evaluated using quantitative polymerase chain reaction. Gene transcripts examined included: thyrotropin-releasing hormone receptor (*trhr*), thyroid-stimulating hormone receptor (*tshr*), sodium-iodide symporter (*nis*), thyroid peroxidase (*tpo*), thyroglobulin (*tg*), transthyretin (*ttr*), deiodinases 1, 2, 3a, and 3b (*dio1, dio2, dio3a* and *3b*), and thyroid hormone receptors alpha and beta (*thr*$\alpha$ and $\beta$). A loess regression method was successful in identifying maxima and minima of transcriptional expression during early development of both species. Overall, we observed great similarities between the species, including maternal transfer, at least to some extent, of almost all transcripts (confirmed in unfertilized eggs), increasing expression of most transcripts during hatching and embryo-larval transition, and indications of a fully functional HPT axis in larvae. These data will aid in the development of hypotheses on the role of certain genes and pathways during development. Furthermore, this provides a background reference dataset for designing and interpreting targeted transcriptional expression studies both for fundamental research and for applications such as toxicology.

**Key Words:** HPT axis, fish, endocrine system, early development, mRNA expression, thyroid hormone

## 1. Introduction

Thyroid hormones (THs) are involved in a variety of biological functions such as growth, morphogenesis, osmoregulation, and skin pigmentation (Blanton and Specker, 2007). The TH, 3,5,3´-triiodothyronine (T4), which is synthesized by thyroid follicle cells, is converted to the more biologically active form, L-thyroxine (T3), via deiodination in peripheral tissues (Fig. 1; Blanton and Specker, 2007; Power et al., 2001; Zoeller et al., 2007). The hypothalamic-pituitary-thyroid (HPT) axis plays a crucial role in the development of teleost fish, including brain development, yolk absorption, body growth and fin differentiation among others (Blanton and Specker, 2007; Power et al., 2001). Previous studies have profiled T4 and T3 levels during early development in fathead minnow and zebrafish (Chang et al., 2012; Crane et al., 2004). However, knowledge of transcription profiles of thyroid-related genes in developing teleosts often is lacking, and what is available generally is fragmented.

In this study, we selected two model teleost species, the fathead minnow (*Pimephales promelas*) and the zebrafish (*Danio rerio*), and constructed detailed transcriptional expression ontogeny profiles relevant to the HPT axis. This enabled comparison of activation of thyroid function during embryo-larval development in the two species. Knowledge gained from this is not only important from the perspective of fundamental developmental biology and comparative physiology, but also for toxicology where both species serve as important animal models. For example, both are commonly used for research with endocrine-disrupting chemicals (EDCs), including those that affect thyroid function (Ankley et al., 2000; Ankley and Villeneuve, 2006; Jensen et al., 2001). Recently, we showed that responses to an environmental thyroid peroxidase (TPO; the enzyme responsible for TH synthesis) inhibitor were highly similar in these two species (Nelson et al., 2016; Stinckens et al., 2016). Thyroid disruption can occur at multiple locations within the thyroid axis, acting through several molecular targets, such as inhibition of T4 production, inhibition of deiodination of T4 to T3 in peripheral tissues, and impacts on TH receptors (Blanton and Specker, 2007). The ontogeny profiles generated in this study could facilitate the identification of molecular targets with special emphasis on their life stage-specificity to aid in ongoing screening and testing efforts for EDCs.

Only limited research has focused on the development of the HPT axis in fathead minnows. Wabuke-Bunoti and Firling (1983) reported the presence of a thyroid anlage at 35 hpf (hours post fertilization) and the first thyroid follicles at 58 hpf, with the first endogenous TH

synthesis observed as early as 1-2 dpf (days post-fertilization) (Fig. 2A; Crane et al., 2004; Devlin et al., 1996; Wabuke-Bunoti and Firling, 1983). While transcriptional changes at specific time points during fathead minnow development following exposure to thyroid-disrupting chemicals have been examined (Cavallin et al., 2017; Nelson et al., 2016), there is little knowledge of thyroid-related transcriptional profiles during normal development. The only report to date is a study in which the expression of TH receptor mRNAs was examined at six time points during fathead minnow development (Johns et al., 2009).

The zebrafish has been proposed as a model for studying vertebrate thyroid development (Heijlen et al., 2013; Wendl et al., 2002), and therefore, more information is available compared to fathead minnow. Figure 2B shows the timing of important thyroid-related and general developmental events for zebrafish (Hagenaars et al., 2014; Kimmel et al., 1995; Porazzi et al., 2009; Stinckens et al., 2016; Villeneuve et al., 2014; Wilson et al., 2012). The presence of the thyroid anlage was shown at about 32 hpf (Opitz et al., 2012), and the first thyroid follicles have been observed at 55 hpf (Alt et al., 2006). The timing of these events is remarkably similar for both species, even though zebrafish hatch around 2.5 dpf compared to 5 dpf for the fathead minnow. For zebrafish, the first endogenous TH production has been reported around 72 hpf (Chang et al., 2012; Elsalini et al., 2003). There have been reports of transcriptional expression of thyroid-related genes during normal zebrafish development including findings from *in situ* hybridization providing information on localization of expression and evidence for maternal transfer of some transcripts (Essner et al., 1997; Takayama et al., 2008). But even for zebrafish, knowledge of thyroid development is limited to a small set of time points, mostly during the first 5 days post-fertilization, and remains fragmented (Alt et al., 2006; Darras et al., 2015; Dong et al., 2013; Essner et al., 1997; Heijlen et al., 2014; Liu and Chan, 2002; Marelli et al., 2016; Opitz et al., 2011, 2012; Thisse et al., 2003; Vatine et al., 2013; Walpita et al., 2007).

The overall objective of the present study was to characterize a comprehensive transcriptional expression ontogeny relevant to the HPT axis in developing fathead minnows and zebrafish. By presenting detailed expression profiles with high resolution in terms of timing and with identification of peaks and lows at specific time points, we aim to compare the activation of the HPT axis and the role of TH in specific developmental phases in these two model species. Additionally, we provide new knowledge on life stage-specific targets of chemicals, and baseline levels for gene expression analyses in fundamental as well as toxicology-oriented research.

## 2. Materials and methods

### 2.1 Organism sampling

#### *2.1.1 Fathead minnow*

Control adult fathead minnows from an in-house culture facility at the US Environmental Protection Agency (USEPA) in Duluth, MN, were used for egg collections. All procedures were conducted in accordance with approved Animal Care and Use Guidelines. UV-treated and filtered Lake Superior Water (LSW) was used for both adult fish and rearing the embryos in flow-through systems. Each adult breeding pair was held in an aquarium containing LSW and a spawning substrate for egg collections. Water temperature was held at 25±1°C, and photoperiod was set at 16:8 light:dark throughout the study. The adult breeders were fed frozen brine shrimp (*Artemia* sp.) to satiation twice daily.

Newly fertilized eggs were collected and pooled from multiple breeding pairs of one male and one female fathead minnow and randomly distributed into egg baskets, which were gently agitated with a rocker system to mimic the natural flow of water over the eggs. The loaded baskets were suspended in fish tanks filled with approximately 10 L of LSW. The LSW was provided at a continuous flow of approximately 45 mL/min to each tank. After all embryos had hatched (after ~120 hpf/5 dpf), they were released from the egg baskets into the tanks with up to 140 larvae/tank, and fed newly-hatched live brine shrimp (*Artemia*, sp.) twice daily.

Embryos/larvae/juveniles were sampled at 24 time points (Table 1), covering the life stages included in the Fish, Early-life Stage Toxicity Test, OECD testing guideline 210 (OECD, 2013). Eight independent biological replicates of 20 embryos each were sampled at the first nine time points. Eight biological replicates of 10-15 larvae each were sampled from 7 until 33 dpf. The sampled fish were anesthetized with buffered tricaine methanesulfonate (MS-222; Finquel, Argent), snap frozen in liquid nitrogen and stored at -80°C until processed.

Table 1: Overview of sampling time points for fathead minnow and zebrafish.

| **Fathead minnow** | | | | **Zebrafish** | | | |
|---|---|---|---|---|---|---|---|
| **Time point** | **hpf** | **dpf** | **dph** | **Time point** | **hpf** | **dpf** | **dph** |
| 1 | 15 | 0.625 | -4.375 | 1 | 1.5 | 0.06 | -2.44 |
| 2 | 24 | 1 | -4 | 2 | 6 | 0.25 | -2.25 |
| 3 | 26 | 1.1 | -3.9 | 3 | 14 | 0.58 | -1.92 |
| 4 | 30 | 1.25 | -3.75 | 4 | 24 | 1 | -1.5 |
| 5 | 50 | 2.1 | -2.9 | 5 | 36 | 1.5 | -1 |
| 6 | 72 | 3 | -2 | 6 | 48 | 2 | -0.5 |
| 7 | 96 | 4 | -1 | 7 | 60 | 2.5 | 0 |
| 8 | 105 | 4.375 | -0.625 | 8 | 72 | 3 | 0.5 |
| 9 | 120 | 5 | 0 | 9 | 84 | 3.5 | 1 |
| 10 | 168 | 7 | 2 | 10 | 96 | 4 | 1.5 |
| 11 | 216 | 9 | 4 | 11 | 120 | 5 | 2.5 |
| 12 | 264 | 11 | 6 | 12 | 144 | 6 | 3.5 |
| 13 | 312 | 13 | 8 | 13 | 192 | 8 | 5.5 |
| 14 | 360 | 15 | 10 | 14 | 240 | 10 | 7.5 |
| 15 | 408 | 17 | 12 | 15 | 288 | 12 | 9.5 |
| 16 | 456 | 19 | 14 | 16 | 336 | 14 | 11.5 |
| 17 | 504 | 21 | 16 | 17 | 384 | 16 | 13.5 |
| 18 | 552 | 23 | 18 | 18 | 432 | 18 | 15.5 |
| 19 | 600 | 25 | 20 | 19 | 480 | 20 | 17.5 |
| 20 | 648 | 27 | 22 | 20 | 528 | 22 | 19.5 |
| 21 | 672 | 28 | 23 | 21 | 576 | 24 | 21.5 |
| 22 | 696 | 29 | 24 | 22 | 624 | 26 | 23.5 |
| 23 | 744 | 31 | 26 | 23 | 672 | 28 | 25.5 |
| 24 | 792 | 33 | 28 | 24 | 720 | 30 | 27.5 |
| | | | | 25 | 768 | 32 | 29.5 |

Hpf: hours post fertilization, dpf: days post-fertilization, dph: days post-hatch

*2.1.2 Zebrafish*

Adult wildtype zebrafish from an in-house laboratory colony maintained in Zebrafishlab at the University of Antwerp (Belgium) were used for egg production. Fish husbandry was carried out in strict accordance with the EU Directive on the protection of animals used for scientific purposes (2010/63/EU). The work was approved by the Ethical Committee for Animals of the University of Antwerp (project number 2015-51) although this was not strictly necessary since the animals have not experienced a level of pain, suffering, distress or lasting harm equivalent to that caused by the introduction of a needle. Reconstituted freshwater (45 mg $l^{-1}$ CaCO3), prepared by adding Instant Ocean® Sea Salt (Blacksburg, VA, US) to reverse osmosis water (Werner, Leverkusen, Germany) up to a conductivity of 500 µS $cm^{-1}$ and adjusting the pH to 7.5 using NaHCO3, was used for both adult fish and rearing the embryos (Hagenaars et al., 2014). Adult fish were kept in a ZebTEC zebrafish housing system (Tecniplast, Buguggiate, Italy) at a 14 h/10 h light/dark cycle, at 28 ± 0.2 °C. The breeding stock was fed three times a day: twice with granulated food (Biogran medium, Prodac International, Cittadella, Italy) at a rate of 0.5% of their mean wet weight and once with thawed and rinsed Artemia sp. nauplii, Daphnia sp., Chironomidae larvae and Chaoboridae larvae alternately.

The night before egg collection, one female and one male zebrafish were separated in breeding tanks with a perforated bottom. The separator was removed when the lights turned on in the morning. Within 45 min of this, eggs were collected and pooled from multiple spawning groups. Embryos were randomly distributed into plastic beakers with an initial loading rate of 45 embryos per 100 ml. The loading rate was gradually decreased to 7 larvae per 100 ml at 10 dpf with gentle aeration initiated at 9 dpf. Solutions were renewed daily. At 15 dpf, larvae were transferred to a ZebTEC zebrafish housing system. Embryos were reared in an incubator at 28.5 °C with a 14 h/10 h light/dark cycle. Fish were fed twice daily with paramecia from 4 to 6 dpf. From 7 to 9 dpf, they were fed paramecia and SDS-100 (Special Diets Services) twice daily. From 10 dpf, they were additionally fed Artemia sp. Nauplii twice daily. Starting at 15 dpf paramecia feeding was reduced to once daily. From 20 to 32 dpf they were fed Artemia sp. nauplii once daily and SDS-100 twice daily.

Embryos/larvae/juveniles were sampled at 25 time points (Table 1). Four independent biological replicates of 30 embryos each were sampled at the first three time points. Four biological replicates of 20 embryos each were sampled from 24 until 84 hpf; on all remaining

time points each of the four replicates comprised 10 organisms. Samples were snap frozen in liquid nitrogen.

For both species whole body samples were collected on each time point. Given the small size of the earliest life stages and the fact that organs have not yet developed at those stages, it was not possible to perform this study on the level of selected organs. Also, the use of whole body samples improves comparability to other studies reporting mRNA levels in fish early life stages, since those studies are confronted with the same technical limitation and therefore commonly report whole body levels. The importance of this fact for correct interpretation of the results is elaborated on in the discussion.

## 2.2 Analysis of mRNA expression

### *2.2.1 Selection of target genes and primers*

The selection of genes was intended to provide a comprehensive coverage of the HPT-axis (Fig. 1), including genes involved in feedback regulation, synthesis, transport, in(activation) and action of THs. We selected well-studied actors in these processes, including known and potential molecular targets of thyroid disrupting chemicals, since for these genes there is a particular need to describe the transcriptional expression ontogeny. The mRNA transcripts examined included 1) thyrotropin-releasing hormone receptor (*trhr*, expressed in the pituitary) and thyroid stimulating hormone receptor (*tshr*, expressed in the follicles of the thyroid gland), which are both involved in HPT-axis mediated feedback regulation of thyroid hormone levels, 2) sodium-iodide symporter (*nis*), thyroid peroxidase (*tpo*) and thyroglobulin (*tg*), which are all expressed in the thyroid follicles and are involved in thyroid hormone synthesis; the sodium-iodide symporter is responsible for uptake of iodide into follicular cells, thyroglobulin is the source of tyrosine residues that are iodinated by the enzyme thyroid peroxidase, 3) transthyretin (*ttr*) which is a plasma protein that transports thyroid hormones and is synthesized by the liver 4), deiodinases 1, 2 and 3 which are involved in activation (main role of *dio1* and *dio2*) and inactivation (main role of *dio3a* and *dio3b*) of thyroid hormones and are expressed in liver and other peripheral tissues, and 5) thyroid hormone receptors alpha and beta (*thr*$\alpha$ and $\beta$), expressed in various TH-responsive tissues and responsible for initiating thyroid hormone action.

For fathead minnow, primers were designed using Integrated DNA Technologies' (IDT) RealTime PCR Tool, such that the amplicons would span two or more exons to reduce the

possibility of contamination of genomic DNA (gDNA) (Table S1). Fathead minnow amplicons were sequenced using Sanger sequencing (University of Minnesota Genomics Center, Minneapolis, MN, USA), and results were confirmed using the National Center for Biotechnology Information's Basic Local Alignment Search Tool (NCBI, BLAST; https://blast.ncbi.nlm.nih.gov/Blast.cgi) to verify alignment with the targeted gene (Table S2). For genes where fathead minnow sequence information was not available from previous studies, the fathead minnow genome browser was utilized to obtain the target sequence information (Saari et al., 2017). The genome browser contains alignment of a fathead minnow SOAPdenovo genome assembly (Burns et al., 2016) to known nucleotide coding sequences in the zebrafish. After the gene-specific fathead minnow sequences were obtained, the coding sequences were confirmed using BLAST to verify alignment with annotated gene sequences in zebrafish (Table S3).

For zebrafish, all primer sequences were obtained from literature (Table S4) and ordered from Eurogentec (Liège, Belgium). Most amplicons spanned two exons. Zebrafish amplicons were sequenced using Sanger sequencing (Genetic Service Facility, University of Antwerp), and results were confirmed using NCBI's BLAST to verify alignment with the targeted gene in the zebrafish genome (Table S2). Due to practical considerations related to primer availability, two different genes for *trhr* were measured in the two model species: *trhr2* for fathead minnow and *trhrb* for zebrafish. For deiodinase 3 (*dio3a* and *dio3b*), we were unable to design successful primers that spanned multiple exons for fathead minnow so these transcripts were only measured in zebrafish.

*2.2.2 Quantification of mRNA levels*

For fathead minnow, total RNA was extracted using RNeasy Micro kits (Qiagen, Hilden, Germany) for pooled embryos and RNeasy Mini Plus kits (Qiagen) for pooled larvae. All samples were DNase-treated using RNase-free DNase (Qiagen) according to the manufacturer's protocol. RNA quality and concentration were determined using a Nanodrop ND-1000 Spectrophotometer (Nanodrop Technologies, Thermo Fisher Scientific, Wilmington, DE). All samples had $A_{260\ nm}/A_{280\ nm}$ ratios > 1.92. Relative transcript abundance of genes was evaluated by qRT-PCR using Power SYBR® Green RNA-to-CT 1-step kits (Applied Biosystems, Foster City, CA, USA). Prior to qRT-PCR, RNA samples were diluted to 10 ng $\mu l^{-1}$. Each qRT-PCR

reaction contained 20 ng total RNA, 9.25 pmol forward primer, and 9.25 pmol reverse primer in a 20 µL volume. The thermocycling program was set to 48°C for 30 min for the reverse transcription step, followed by 95°C for 10 min, and 40 cycles of 95°C for 15 s and 60°C for 1 min for PCR amplification, and a dissociation stage of 95°C for 15 s, 60°C for 1 min, and 95°C for 15 s. Relative transcript abundance of each gene was quantified relative to gene-specific mRNA or cDNA duplicate standard curves with six concentrations, in a 10-fold dilution series (2 x $10^7$ to 200 copies $\mu l^{-1}$). Standards were prepared through a series of cDNA amplifications as described by Villeneuve et al. (2007). Melting curves were assessed to confirm specific amplification. *Rp18* and *bactin*, were selected from three potential reference genes (Table S1), using a set of Excel macros, geNorm (Vandesompele et al., 2002). The transcript abundance of each sample was divided by the geometric mean of *rp18* and *bactin* transcript abundances in that sample to normalize the experimental data for reference gene expression (Vandesompele et al., 2002). The resulting data were divided by the average abundance at the time point with the lowest expression for each gene, and subsequently log2 transformed to increase the resolution. All graphs show log2 relative quantities which have been normalized for reference gene expression and expressed relative to the time point with the lowest expression. This means that a log2 relative quantity of 2 for a particular time point corresponds to 4 times the expression of the time point with the lowest expression.

For zebrafish, RNA was extracted using the Nucleospin® RNA isolation kit (Macherey-Nagel, Düren, Germany) according to the manufacturer's instructions, including a DNAse treatment. RNA purity and integrity were confirmed using a NanoDrop spectrophotometer and a BioAnalyzer (Agilent Technologies, Diegem, Belgium). All samples had minimal $A_{260\ nm}/A_{280\ nm}$ ratios of 2.1 and minimal RIN (RNA integrity number) of 7.9. cDNA was constructed using a Revertaid H Minus First Strand cDNA Synthesis Kit (Thermo Fischer Scientific, Waltham, MA, USA) according to the manufacturer's instructions, with random hexamer primers. Relative transcript abundance of genes was evaluated by qPCR in an MX3005P (Agilent Technologies) using the Brilliant II SYBR® Green qPCR Master Mix (Agilent Technologies). cDNA was diluted to 70 ng $\mu l^{-1}$ and each qPCR reaction contained 350 ng cDNA, 10 pmol forward primer, and 10 pmol reverse primer in a final volume of 19.3 µL. Thermal cycling profiles were: an initial denaturation period of 10 min at 95°C, followed by 40 cycles of 20 s at 95°C, 40 s at 55°C (58°C for *dio2*) and 30 s at 72°C. Melting curves were assessed to confirm specific

amplification. Primer efficiencies were determined in each run using duplicate standard curves of four sequential dilutions of a mixed sample based on different time points. *18S* and *actb1* were selected from five potential reference genes (Table S4), using geNorm (Vandesompele et al., 2002). Transcript abundances were normalized with the geometric mean of the two reference genes identical to fathead minnow data, and an inter-run calibration was performed using qbase+ software, version 3.1 (Biogazelle, Zwijnaarde, Belgium - www.qbaseplus.com). Identical to the fathead minnow, data are shown as log2 relative quantities which have been normalized for reference gene expression and expressed relative to the time point with the lowest expression. These data are also used in subsequent statistical analyses.

*2.3 Confirmation of maternal transfer*

To test whether mRNA transcripts were maternally transferred to eggs, a set of experiments was conducted in which transcript abundance was compared between unfertilized and fertilized fathead minnow and zebrafish eggs. For fathead minnows, we used an *in vitro* fertilization technique to obtain samples for this analysis. Sexually mature males and females were paired with a spawning substrate, observed for spawning behavior, and collected upon spawning behavior initiation (ready to spawn, but had not spawned yet). The fish were anesthetized in MS-222 prior to sperm and egg collection. Sperm was collected into capillary tubes, transferred to Hank's solution, and pooled from several males. Eggs were collected by gently squeezing the abdomen of each female and releasing the eggs onto glass microscope slides covered with control LSW. A subset of 20 unfertilized eggs was collected from each female and immediately snap frozen in liquid nitrogen. The remaining eggs were fertilized by gently transferring the pooled sperm onto the glass slides containing eggs. The eggs were allowed to develop for 1.5 hpf after which a subset of 20 fertilized eggs were collected from each female and snap frozen in liquid nitrogen. A total of seven matched unfertilized and fertilized fathead minnow egg samples were collected and used in subsequent qRT-PCR analyses.

For zebrafish, eight breeding pairs were isolated, and eggs were collected after the lights were turned on. The eggs were separated into groups of unfertilized and fertilized eggs based on visual confirmation under a stereomicroscope. Eggs that were still in the 1-cell stage at 1.5 hpf were placed in the unfertilized group, while eggs showing clear cell divisions were placed in the fertilized group. Pools of 30 unfertilized and 30 fertilized eggs were collected from each of the

eight pairs. Samples were snap frozen in liquid nitrogen after 1.5 hpf. A total of eight matched unfertilized and fertilized zebrafish egg samples were analyzed by qPCR.

The samples were processed and analyses of mRNA levels for all thyroid-related and reference genes were conducted as described under 2.2.2. A subset of samples from the original ontogeny sample set was included in the measurements for each gene to allow adjustment for possible plate-to-plate variation between the maternal transfer test and the ontogeny study, with a set of samples from the earliest time point (15 hpf for fathead minnows; 1.5 hpf for zebrafish) as well as the point of immediate lowest expression for transcripts showing an initial decrease in the ontogeny profile, or a point at which expression has increased for transcripts showing an immediate increase in the ontogeny profile. The ratio between the ontogeny sample data and the maternal transfer data was calculated (before log2 transformation) and used as an adjustment factor for the unfertilized egg data to compare between the two PCR analyses.

*2.4 Statistical analysis*

Log2 relative quantities from both species were analyzed using R Statistical Software (R Core Team, 2016 version 3.2.0, https://www.R-project.org/). The R code used in the analyses is described in the Supplementary information (Supplement 4). The aim of the analysis was to determine when the trend in mRNA expression data started to deviate significantly. This is accomplished by determining when the derivative of the best fit function through the data equals 0, thereby defining critical points (e.g., local maxima and minima) of mRNA expression. Since the trends in response for each gene are largely non-linear, the best fit function through the data is determined by using local regression (loess). The span used in loess was determined by using the span that produced the simplest model within 3.8 AIC (Akaike information criterion; Akaike, 1974) of the span that produced the model with the lowest AIC. Selection of the loess model was verified by confirming that the residuals had no pattern over time. Critical points (i.e., minima, maxima, and inflection points) in the data were calculated using the first derivative (which is calculated using Newton's difference quotient) of the estimated best-fit curve. To account for the variability in the data, best fit functions are re-estimated on resampled data using parametric bootstrapping. The quantile ranges of the derivatives of re-estimated best fit functions are then used to determine the confidence intervals of the derivatives of the estimated best fit function at

each time. When the confidence intervals of the derivatives of the estimated best fit function contain 0 at a specific time, that specific time is considered to be a critical point.

Log2 relative quantities from the maternal transfer study were analyzed using a paired t-test ($p<0.05$; GraphPad Prism v. 5.02) to assess statistical differences between unfertilized eggs and fertilized eggs, by matching them based on the same breeding couple. The data from unfertilized eggs were plotted on the ontogeny figures (Figs. 3-7) after adjusting for plate-to-plate variation using a subset of samples from two time points which were analyzed in both the maternal transfer test and ontogeny study.

A principal component analysis (PCA) was performed on the 10 transcripts that were measured in both species. Data from 21 time points that were similar in both species were selected to ensure equal contribution of different ages to the patterns for both species. The function 'prcomp' in R was used with scaling. A biplot showing the positions of the time points as a function of the first and second principal component was constructed. The time points were connected to show a species-specific path. Pearson correlation tests were performed on data from all transcripts at all time points using the function 'cor.test' of the 'stats' package and the results were visualized as a correlation matrix using the function 'corrplot' of the 'corrplot' package (https://CRAN.R-project.org/package=corrplot). Both intra-species and inter-species transcript correlation analyses were conducted in this manner.

## 3. Results & Discussion

The loess regression method was successful in identifying key inflection points (i.e., local maxima and minima) of transcriptional expression during early development of both species resulting in the identification of statistically significant highs and lows in the profiles (Figs. 3-7). Data are reported as log2 relative quantities (relative to the time point with the lowest expression) and should therefore not be used for direct comparison of absolute expression levels among transcripts or species.

The ontogeny profiles suggest maternal transfer of transcripts, especially for those transcripts showing relatively high initial levels of expression. Since conclusive evidence of maternal transfer can only be demonstrated using unfertilized eggs, we directly compared transcript levels in unfertilized and fertilized eggs at 1.5 hpf. For zebrafish, the eggs were

separated into groups of unfertilized and fertilized eggs based on visual confirmation under a stereomicroscope. For the fathead minnow, *in vitro* fertilization was employed. Since these data were obtained in separate experiments, they were not included in the overall analysis of the ontogeny profiles, but rather are shown as separate points on the ontogeny graphs (asterisks in Figs. 3-7). The analysis of unfertilized eggs confirmed the presence of all transcripts in both species, except for *trhr* and *tshr* in zebrafish (the 1.5 hpf time point is absent in Fig. 3C and Fig. 3D), although much more pronounced for some transcripts than for others. For the latter we could not derive a Ct value, even after increasing the number of cycles in the qPCR to 45. Additionally, for fathead minnow the presence of transcripts in unfertilized eggs showed that maternal transfer was initially often underestimated based on the earliest time point in the ontogeny study which was not until 15 hpf.

We observed marked changes in expression of thyroid-related gene transcripts during specific phases of development, confirming that the timing of TH synthesis and activation is tightly controlled during early development. The development of the HPT axis in both species as it relates to transcript expression is subsequently discussed in detail by focusing on specific phases of development as shown by the color bars in the ontogeny profiles (Figs. 3-7). Further, an overall inter-species and intra-species comparison of the profiles is presented.

*3.1 Maternal transfer and activation of the HPT axis during embryonic development*

Previous studies have determined that during fish embryonic development, thyroid hormones are obtained by maternal transfer to the yolk sac (Power et al. 2001), and this has been suggested for both fathead minnow (Crane et al., 2004) and zebrafish (Chang et al., 2012). There is limited information, however, on maternal transfer of thyroid-related transcripts in the literature. While Essner et al. (1997) and Takayama et al. (2008) confirmed maternal transfer of mRNA coding for different *thrα* isoforms in unfertilized zebrafish eggs, most reports are based on zebrafish embryos in the 1- or 2-cell stage. For example, Dong et al. (2013) showed *dio1* and *dio2*, but not *dio3* mRNA expression from the 2-cell stage onwards using whole mount *in situ* hybridization. For the first time, we unambiguously show a comprehensive overview of maternal transfer of thyroid-related transcripts in unfertilized zebrafish and fathead minnow eggs.

We detected maternal transfer (in unfertilized eggs, asterisks in Figs. 3-7) for all thyroid-related transcripts in fathead minnow, and for all but two transcripts (*trhr* and *tshr*, Fig. 3), in

zebrafish. We did not observe any differences between mRNA levels in unfertilized and fertilized eggs, suggesting that fertilized eggs at 1.5 hpf are useful to study maternal transfer (Fig. S1). Previous research has shown that zebrafish knockdowns of the deiodinases and the thyroid receptors impaired development of the brain, eye and ear and the first signs of morphological defects could already be observed within 24 hours, confirming that thyroid hormones are essential for the earliest phases of embryonic development (Houbrechts et al., 2016; Marelli et al., 2016; Walpita et al., 2009). The absence of maternal *trhr* and *tshr* transcripts in unfertilized zebrafish eggs could indicate that at this point feedback mechanisms for regulating TH synthesis are not yet functional.

Apart from the absence of maternal transfer, we observed two distinct patterns of maternal transfer and subsequent endogenous synthesis of transcripts (Table 2), and this was highly similar for 6 out of the 10 genes that could be directly compared between the two species (first row in Table 2). For the first pattern, we observed a high level of maternal mRNA that was gradually degraded during early embryonic development, before endogenous mRNA synthesis resulted in increasing levels, usually around 1-2 dpf. This pattern was observed for the main genes essential for thyroid hormone synthesis, activation, and action, in both species: *nis* and *tpo* which are directly involved in TH synthesis (Fig. 4), *dio2* which is involved in TH activation (Fig. 6), and the thyroid hormone receptors which are required to produce target tissue responses (Fig. 7). Several genes showed a second pattern with limited maternal transfer followed by the onset of endogenous synthesis immediately after the embryonic genome was activated in the blastula period (2.25-5.25 hpf in zebrafish, Wragg and Müller, 2016; no details are available for fathead minnow), resulting in a steep and early increase of mRNA levels (Table 2). Interestingly, *ttr*, coding for a transporter of TH in the blood plasm, showed a distinct profile, different from all other transcripts, with an increase up to levels typical for later ages by 24 hpf in fathead minnow but not in zebrafish (Fig. 5B, 5D). In a previous report, the first expression of *tg* mRNA in zebrafish was observed at 34 hpf (Alt et al., 2006), while our dataset shows increasing *tg* mRNA levels already at 6 hpf, immediately after activation of the embryonic genome (Fig. 5C). Transcript levels of *dio1* and *dio3a/b* also increased immediately in zebrafish (Fig. 6C, 6E, 6F, pattern 2 in Table 2), while *dio2* transcript levels increased only after 1-2 dpf (Fig. 6D, pattern 1 in Table 2). Based on knockdown studies targeting the specific deiodinase isoforms, it has been previously suggested that *dio1* is not essential for normal embryonic development in the absence

of other TH disruptions (Darras et al., 2015), while knockdown of *dio2* and *dio3b* resulted in apparent developmental defects (Bagci et al., 2015; Walpita et al., 2009). Taken together, this suggests that neither of the early expression patterns is exclusively linked to transcripts that are essential for normal embryonic development.

Although 4 out of 10 genes that could be directly compared between species were categorized under different expression patterns, for most of these genes, the observed differences were limited (Table 2, Figs. 3-7). Early expression patterns of *trhr* were in fact quite similar, in both species initial expression was absent or very low and showed an early increase. In this context, it should be noted that the current dataset is limited to transcript levels which are not necessarily linearly related to protein levels. Therefore, at this point it is difficult to conclude whether these very low early expression levels, and the small differences between species, are functionally relevant. For *tg* in fathead minnow, the pattern of high maternal transfer with subsequent mRNA degradation was not very pronounced when compared to *nis* or *tpo*. For *tshr* and *dio1*, we did see higher maternal transfer in fathead minnow compared to zebrafish. The latter could reflect cross-species differences in the importance of specific deiodinase isoforms during particular stages of development, but this requires further investigation on the functional level, for example, using deiodinase knockdowns in fathead minnow.

Overall, both expression patterns (Table 2) resulted in the presence of thyroid-related transcripts during the earliest phases of embryonic development, suggesting that not all T4 present during embryonic stages is derived from maternal sources and that there is a need for early embryonic TH production before the appearance of thyroid follicles in both species (Tf in Figs. 3-7). Again, the study of protein levels and/or enzyme activity levels would shed further light on this.

Table 2: Overview of patterns of maternal transfer and subsequent endogenous transcription

| | **Pattern 1: high maternal transfer with subsequent mRNA degradation** | **Pattern 2: limited maternal transfer with immediate onset of endogenous synthesis** | **No maternal transfer** |
|---|---|---|---|

| | | | |
|---|---|---|---|
| **both species** | *tpo, nis, dio2, thrα, thrβ* | *ttr* | - |
| **fathead minnow** | *tshr, tg, dio1* | *trhr2* | - |
| **zebrafish** | - | *tg, dio1, dio3a, dio3b* | *trhrb, tshr* |

The hypothesis that not all T4 present during embryonic stages is from maternal sources is supported by a previous study conducted by Crane et al. (2004) in which fathead minnow whole body T4 and T3 concentrations increased during embryonic development. A significant increase was already observed between 1 and 2 dpf, which corresponds to the appearance of the thyroid anlage at 35 hpf prior to the first observation of thyroid follicles at 58 hpf (Fig. 2; Wabuke-Bunoti and Firling, 1983). For zebrafish, the first clear evidence of endogenous production of TH was found only by about 3 dpf (Chang et al., 2012; Elsalini et al., 2003), while the thyroid anlage appears around 32 hpf comparable to fathead minnows. However, the data of Chang et al. (2012) and Walpita et al. (2007) showed non-significant increases of TH levels between 1 and 2 dpf. In the present study, maternal transfer of *nis* and *tpo* was markedly elevated in both species, and in zebrafish in particular, levels of *tg* increased before the appearance of the thyroid anlage at 32-35 hpf. Given these lines of evidence and the similarities to fathead minnow, it seems plausible that zebrafish endogenous TH production is also initiated around 1-2 dpf. It currently remains unclear whether TH-driven regulation of embryonic development relies completely on maternally transferred thyroid hormones and when embryonic TH production is initiated in zebrafish. This uncertainty warrants a more detailed study of TH levels at these early stages in zebrafish, perhaps combined with a statistical analysis similar to the present study to enable identification of the earliest endogenous TH production.

Walpita et al. (2007) showed that T3 supplementation accelerated hatching in zebrafish, indicating that TH signals are needed to induce hatching. Most transcripts in our study showed increasing levels during the time of hatch in both species (H indicated on the X-axis in Figs. 3-7). *Nis* and *tpo* showed a more gradual increase in mRNA levels, possibly reflecting thyroid cell proliferation, which in zebrafish only starts around 72 hpf (Alt et al., 2006). *Tg*, *ttr* and *dio1* showed rather stable transcript levels in fathead minnow at the time of hatch, while these transcripts were still in their early increase in zebrafish. This could be explained by the difference in timing of hatching between the two species. While several developmental events, including the appearance of neuromeres, the thyroid anlage, circulation, the first thyroid follicles,

the gill anlagen and the complete absorption of the yolk align very well between the two species, zebrafish hatch by 48-72 hpf while fathead minnows do not hatch until 5 dpf (Fig. 2). Therefore, it seems that fathead minnows are morphologically further developed by the time they hatch.

*3.2 HPT axis functionality during embryo-larval transition*

During early development, fish undergo an embryonic-to-larval transition phase marking an important switch from yolk sac to exogenous feeding larvae (green to blue gradient in Figs. 2-7). This transition is known to depend on TH activity and includes inflation of the posterior swim bladder, structural and functional maturation of the mouth and gastrointestinal tract, and resorption of the yolk sac (Liu and Chan, 2002). This transition phase occurs around 6-9 dpf for fathead minnow and 4.5-7 dpf for zebrafish (Figs. 2-7). We previously showed that disruption of TH levels during embryonic development interferes with normal inflation of the posterior swim bladder chamber after combined knockdown of *dio1* and *dio2* or knockdown of *dio3b* in zebrafish (Bagci et al., 2015), and exposure to a model deiodinase inhibitor in fathead minnow (Cavallin et al., 2017). In both fathead minnow and zebrafish, we observed a peak in the transcript levels of *dio1* and in zebrafish we additionally observed a peak of *dio2* and *dio3b* mRNA levels at the time of posterior swim bladder chamber inflation (Psb in Fig. 6). Dong et al. (2013) also found that *dio1* and *dio2* are specifically expressed in the zebrafish swim bladder tissue at 96 hpf, confirming their role in swim bladder inflation. In both species, most of the other studied transcripts showed either a peak in expression during the embryo-larval transition or an increase throughout that period, suggesting that early larvae are capable of producing TH, and further reflecting the importance of the thyroid pathway in this developmental event. Chang et al. (2012) reported a corresponding increase in T4 and T3 levels with a peak at 5 dpf in zebrafish. For the fathead minnow, a rapid increase in TH concentrations was observed immediately following hatch during the embryo-larval transition (Crane et al., 2004).

*3.3 HPT axis functionality during larval development*

By the time the embryo-larval transition is completed, around 9 dpf for fathead minnow and 7 dpf for zebrafish (start of the light blue larval phase in Figs. 2-7), the period of marked transcriptional increases has ended and most transcripts have reached high levels of expression, including *trhr* and *tshr* (Fig. 3). At this point, based on these transcriptional patterns, the HPT

axis has potential to be fully functional in both species. Thereafter (remainder of light blue larval phase in Figs. 2-7), several transcripts start to level out, while others even show decreasing expression (*dio3a/3b*), suggesting TH homeostasis and a reduced need for TH as a driver of development in this time frame.

*3.4 HPT axis functionality during larval-juvenile transition*

During late larval development, fish undergo a larval-to-juvenile transition which is also known to be stimulated by TH, including the formation of scales and the development of the adult pigment pattern and fin morphology (Brown, 1997; Liu and Chan, 2002). For fathead minnow this transition occurs around 14-23.5 dpf and for zebrafish around 20-30 dpf (light blue to dark blue gradient in Figs. 2-7). For both species this also includes anterior swim bladder chamber inflation, which occurs around 14 dpf in fathead minnow and around 20 dpf in zebrafish (Asb in Figs. 3-7). While we observed stable expression of many transcripts in this period, there were also some transcriptional changes associated with this time frame. In zebrafish we observed a slight increase of *ttr* mRNA levels suggesting an increased need for circulating TH (Fig. 5). While deiodinase mRNA levels remained stable during this time in fathead minnow, we observed increased transcript levels of *dio2* at 20 dpf and a slight increase of *dio1* mRNA in zebrafish (Fig. 6), suggesting an increased need for activation of T4 to T3. The coinciding low levels of *dio3a* and *dio3b* mRNA suggest reduced inactivation of T3. For fathead minnow we have previously shown that anterior inflation is impaired by deiodinase inhibition during the larval period (Cavallin et al., 2017), confirming the role of the deiodinases in this process. While an increased T3/T4 ratio would be expected based on the deiodinase transcriptional expression pattern, Chang et al. (2012) observed an increase of T4 but not T3 in zebrafish. However, in fathead minnow, Crane et al. (2004) did observe increased levels of T3 at the time of anterior chamber inflation. For correct interpretation of these results, it is important to note that both the transcript levels reported in the current study as well as the TH levels reported in the studies of Chang et al. (2012) and Crane et al. (2004) are whole body levels. It seems plausible that when the HPT axis is fully functional, TH-driven developmental events rely more on localized expression changes than on whole body mRNA/protein levels. There was an increase of whole body T4 at the time of anterior chamber inflation in the zebrafish (Chang et al. 2012), which could be activated to T3 specifically in swim bladder tissues. This is in line with the decreased

transcript levels of *trhrb* and *tshr* around the same time point in this study, since the hypothalamus-pituitary feedback system responds to circulating TH levels and not to local tissue levels. The hypothesis that developmental events may rely on localized expression of transcripts is in line with reports of *dio1* and *dio2* mRNA expression as well as the TH receptors specifically in swim bladder tissue around the time of posterior chamber inflation shown by *in situ* hybridization (Dong et al., 2013; Marelli et al., 2016). There are currently no reports of similar evaluations later during larval and juvenile development.

Although it is well-known that thyroid hormones are important for larval-to-juvenile transition and we previously showed that Tpo inhibition impaired anterior chamber inflation in both species (Nelson et al., 2016; Stinckens et al., 2016), zebrafish tpo mRNA levels were markedly decreased around 20 dpf (Fig. 4), suggesting a possible activity decrease of thyroid synthesis. Again, the fact that whole body samples were used could be important for interpreting this result. The decline in *tpo* mRNA expression may be explained by dilution of the gene transcripts given that the relative size of the thyroid may decrease in proportion to the increasing body mass as the larvae mature (i.e. allometric relation between organ and body growth). The decreasing levels of *nis* and *tpo* transcripts in juvenile fathead minnows could be similarly caused by growth (dark blue phase in Fig. 4). Additionally, as mentioned earlier, protein levels are often not linearly related to transcript levels, and altered translation rates could for example play a role. This provides a good illustration of how changes in mRNA expression can help build hypotheses and point out interesting time points where the focused study of protein levels, enzyme activity and thyroid hormone levels may provide further insight into the underlying mechanisms of known developmental events.

*3.5 Inter-species and intra-species comparison of expression profiles*

We performed a PCA to generate a summary of all data from all transcripts for both species. The biplot in Fig. 8 presents the time-dependent path of each species in the complete space of transcriptional expression changes. The two species followed similar paths except for the late-larval and juvenile time points where there was some divergence. Almost all of the genes had a strong positive correlation with the first principal component (PC1) which accounts for 64% of the variation in the data, while *tpo* had a strong negative correlation with PC2 which accounts for 11% of the variation in the data (Fig. S2A). The tendency of the paths of both

species to move from the left to the right on the plot therefore reflects a gradual increase of transcript levels during development. The move into the lower right quadrant (negative values on PC2) that both species show in the embryo-larval transition mainly reflects the increasing *tpo* transcript expression, which is probably a good proxy for thyroid gland maturation. The late larval difference between the paths of the two species is partly driven by differences in *tpo* mRNA expression in this period. While in the fathead minnow, *tpo* transcript levels markedly decrease, expression in zebrafish increased again after the low around the time of anterior swim bladder inflation. The movement of the path of fathead minnows to negative values on PC1 reflects our observation that several transcripts in the fathead minnow showed such a decrease in the late-larval period. The physiological consequences of these differences are unclear at this point. An inter-species correlation analysis confirmed that most transcripts are highly correlated between the two species, except for *tpo* and *tg*, the main genes important for TH synthesis (Fig. S2B).

Intra-species correlation analyses showed that most genes have very similar profiles, while again *tpo*, and *tg* (for fathead minnow, Fig. S2C) or *nis* (for zebrafish, Fig. S2D), showed strongly deviating trends. This again indicates distinct patterns for genes involved in TH synthesis versus non-synthetic genes in the thyroid pathway. While most transcripts were maternally transferred to some extent, especially for *tpo* and *nis* we observed high maternal transfer followed by dramatic RNA degradation. Note that Figs. 4A and 4B show that the extent of maternal transfer of *tpo* and *nis* in fathead minnow was even greater than what was initially reflected given the earliest time point in the ontogeny study was not until 15 hpf.

## 4. Conclusions

Even though zebrafish hatch 2.5 days earlier than fathead minnows, the timing of events essential to the formation and function of the thyroid gland is very similar between both species. The PCA summarizing all transcriptional profiles showed a high similarity of the time-dependent transcriptional changes during development of both species during the embryo-larval period while it showed a diverging pattern in the late-larval and juvenile stage. A correlation analysis further demonstrated that, on the level of the individual genes, the profiles were highly similar, with exceptions especially noted for genes directly involved in the synthesis of TH. Important similarities included maternal transfer of almost all transcripts, increasing expression of most

thyroid-related transcripts throughout the period of hatching and embryo-larval transition, and indications of a fully functional HPT axis during the larval period. Additionally, in previous studies, we have shown that responses of both species to thyroid hormone disruption were very similar. This further strengthens the idea that both from a fundamental and toxicological perspective, knowledge from the two species can be combined and interpreted on the same grounds.

This dataset is part of a larger effort in describing transcriptional expression patterns of genes involved in several processes of interest during embryo-larval development. Follow-up papers will include reports on profiles of genes involved in the steroid hormone biosynthesis pathway, biotransformation and digestion. By making these data available, we aim to aid in the development of hypotheses on the role of certain genes and pathways during development. Interactive graphs of the ontogeny data are available on our website (http://zebrafishlab.be/ontogeny-explorer). Furthermore, this dataset can function as a background reference for designing and interpreting targeted transcriptional expression studies both for fundamental research and for applications such as toxicology, for instance by aiding in the selection of relevant time points.

## 5. Acknowledgements

The authors thank Kevin Lott (Badger Technical Services) for additional technical support. We also thank Dr. Jennifer Olker for providing helpful review comments on an earlier draft of this manuscript. This article has been reviewed in accordance with official U.S. EPA policy. Mention of products or trade names does not indicate endorsement or recommendation for use. Conclusions drawn in this study neither constitute nor reflect the views or policies of the U.S. EPA.

## 6. Competing interests

No competing interests declared.

## 7. Funding

This work was supported by the European Chemical Industry Council (Cefic) Long-range Research Initiative (LRI-ECO20 and LRI-ECO20.2) with support of ECETOC, by the Belgian

Federal Public Service of Health, Food chain safety and Environment (TRANSGGO), and by Universiteit Antwerpen (BOF-KP 2015 ID 31088 and DOCPRO 2015-2019 ID 31405). Lucia Vergauwen was supported by the LRI-ECO20 and LRI-ECO20.2 projects. The USEPA authors' contributions were supported by the Chemical Safety for Sustainability research program. The funding sources were not involved in study design; in the collection, analysis and interpretation of data; in the writing of the report; and in the decision to submit the article for publication

## 8. Data availability

The zebrafish cDNA library is available upon request, and all zebrafish and fathead minnow data are available through data.gov (search by article title and/or author names) and via interactive graphs on our website (http://zebrafishlab.be/ontogeny-explorer).

## 9. References

Akaike, H., 1974. A new look at the statistical model identification. IEEE Trans. Automat. Contr. 19(6), 716-723.

Alt, B., et al., 2006. Analysis of origin and growth of the thyroid gland in zebrafish. Dev. Dynam. 235, 1872-1883.

Ankley, G.T., et al., 2000. Description and evaluation of a short-term reproduction test with the fathead minnow (*Pimephales promelas*). Environ. Toxicol. Chem. 20, 1276-1290.

Ankley, G.T., Villeneuve, D.L., 2006. The fathead minnow in aquatic toxicology: Past, present and future. Aquat. Toxicol. 78, 91-102.

Bagci, E., et al., 2015. Deiodinase knockdown during early zebrafish development affects growth, development, energy metabolism, motility and phototransduction. PLoS ONE 10, e0123285.

Baumann, L., et al., 2016. Thyroid disruption in zebrafish (*Danio rerio*) larvae: Different molecular response patterns lead to impaired eye development and visual functions. Aquat. Toxicol. 172, 44-55.

Biga P.R., et al., 2005. The isolation, characterization, and expression of a novel GDF11 gene and a second myostatin form in zebrafish, *Danio rerio*. Compar. Biochem. Physiol. B 141(2), 218-230.

Blanton, M.L., Specker, J.L., 2007. The hypothalamic-pituitary-thyroid (HPT) axis in fish and its role in fish development and reproduction. Crit. Rev. Toxicol. 37, 97-115.

Brown, D. D., 1997. The role of thyroid hormone in zebrafish and axolotl development. Proc. Natl. Acad. Sci. USA. 94, 13011-13016.

Burns, F.R., et al., 2016. Sequencing and de novo draft assemblies of a fathead minnow (*Pimephales promelas*) reference genome. Environ. Toxicol. Chem. 35, 212-217.

Cavallin, J.E., et al., 2017. Impaired swim bladder inflation in early-life stage fathead minnows exposed to a deiodinase inhibitor, iopanoic acid. Environ. Toxicol. Chem. DOI: 10.1002/etc.3855.

Chang, J., et al., 2012. Changes in thyroid hormone levels during zebrafish development. Zoolog. Sci. 29, 181-184.

Crane, H.M., et al., 2004. Developmental changes of thyroid hormones in the fathead minnow, *Pimephales promelas*. Gen. Comp. Endocrinol. 139, 55-60.

Darras, V.M., Houbrechts, A.M., Van Herck, S.L.J., 2015. Intracellular thyroid hormone metabolism as a local regulator of nuclear thyroid hormone receptor-mediated impact on vertebrate development. Biochim. Biophys. Acta. 1849, 130-141.

Devlin, E.W., et al., 1996. Prehatching development of the fathead minnow *Pimephales promelas* rafinesque. EPA/600/R-96/079.

De Wit M., et al, 2008. Molecular targets of TBBPA in zebrafish analysed through integration of genomic and proteomic approaches. Chemosphere 74(1), 96-105.

Dong, W., et al., 2013. Using whole mount in situ hybridization to examine thyroid hormone deiodinase expression in embryonic and larval zebrafish: A tool for examining OH-BDE toxicity to early life stages. Aquat. Toxicol. 132-133, 190-199.

Elsalini, O.A., et al., 2003. Zebrafish hhex, nk2.1a, and pax2.1 regulate thyroid growth and differentiation downstream of Nodal-dependent transcription factors. Dev. Biol. 263, 67-80.

Essner, J.J., et al., 1997. The zebrafish thyroid hormone receptor α1 is expressed during early embryogenesis and can function in transcriptional repression. Differentiation 62, 107-117.

Filby, A.L., Tyler, C.R., 2007. Appropriate 'housekeeping' genes for use in expression profiling the effects of environmental estrogens in fish. BMC Mol. Biol. 8:10. Doi: 10.1186/1471-2199-8-10.

Gonzalez P., et al., 2006. Comparative effects of direct cadmium contamination on gene expression in gills, liver, skeletal muscles and brain of the zebrafish (*Danio rerio*). BioMetals 19, 225-35.

Hagenaars, A., et al., 2014. PFOS affects posterior swim bladder chamber inflation and swimming performance of zebrafish larvae. Aquat. Toxicol. 157, 225-235.

Heijlen, M., Houbrechts, A.M., Darras, V.M., 2013. Zebrafish as a model to study peripheral thyroid hormone metabolism in vertebrate development. Gen. Comp. Endocrinol. 188, 289-296.

Heijlen, M., et al., 2014. Knockdown of type 3 iodothyronine deiodinase severely perturbs both embryonic and early larval development in zebrafish. Endocrinol. 155, 1547-1559.

Houbrechts A.M., et al., 2016. Deiodinase knockdown affects zebrafish eye development at the level of gene expression, morphology and function. Mol. Cell. Endocrinol. 424(C), 81-93.

Jensen, K.M., et al., 2001. Aspects of basic reproductive biology and endocrinology in the fathead minnow (*Pimephales promelas*). Comp. Biochem. Physiol. C: Toxicol. Pharmacol. 128, 127-141.

Johns, S.M., et al., 2009. Characterization of ontogenetic changes in gene expression in the fathead minnow (*Pimephales promelas*). Environ. Toxicol. Chem. 28, 873-880.

Kimmel, C.B., et al., 1995. Stages of embryonic development of the zebrafish. Dev. Dynamics. 203, 253-310.

Liu, C.S., Yu, H.X., Zhang, X.W., 2013. Zebrafish embryos/larvae for rapid determination of effects on hypothalamic-pituitary-thyroid (HPT) and hypothalamic-pituitary-interrenal (HPI) axis: mRNA expression. Chemosphere 93(10), 2327-2332.

Liu, Y.-W., Chan, W.-K., 2002. Thyroid hormones are important for embryonic to larval transitory phase in zebrafish. Differentiation 70, 36-45.

Liu Y., et al., 2011. The thyroid-disrupting effects of long-term perfluorononanoate exposure on zebrafish (*Danio rerio*). Ecotoxicology 20(1), 47-55.

Marelli, F., et al., 2016. Patterns of thyroid hormone receptor expression in zebrafish and generation of a novel model of resistance to thyroid hormone action. Mol. Cell. Endocrinol. DOI: 10.1016/j.mce.2016.01.020.

Nelson, K.R., et al., 2016. Impaired anterior swim bladder inflation following exposure to the thyroid peroxidase inhibitor 2-mercaptobenzothiazole part I: fathead minnow. Aquat. Toxicol. 173, 192-203.

Noyes, P.D., et al., 2013. Low level exposure to the flame retardant BDE-209 reduces thyroid hormone levels and disrupts thyroid signaling in fathead minnows. Environ. Sci. Technol. 47: 10012-10021.

OECD, 2013. Test No. 210: Fish, Early-life Stage Toxicity Test, OECD Guidelines for the Testing of Chemicals. doi; 10.1787/9789264203785-en.

Opitz, R., et al., 2011. TSH receptor function is required for normal thyroid differentiation in zebrafish. Mol. Endocrinol. 25, 1579-1599.

Opitz, R., et al., 2012. Transgenic zebrafish illuminate the dynamics of thyroid morphogenesis and its relationship to cardiovascular development. Dev. Biol. 372, 203-216.

Pinto P.I.S., Guerreiro E.M., Power D.M., 2013. Triclosan interferes with the thyroid axis in the zebrafish (*Danio rerio*). Toxicol. Res. 2(1), 60-69.

Porazzi, P., et al., 2009. Thyroid gland development and function in the zebrafish model. Mol. Cell. Endocrinol. 312, 14-23.

Power, D.M., et al., 2001. Thyroid hormones in growth and development of fish. Comp. Biochem. Physiol. C Toxicol. Pharmacol. 130, 447-459.

Saari, T., et al., 2017. First generation annotations for the fathead minnow (*Pimephales promelas*) genome. Environ. Toxicol. Chem. DOI: 10.1002/etc.3929.

Stinckens, E., et al., 2016. Impaired anterior swim bladder inflation following exposure to the thyroid peroxidase inhibitor 2-mercaptobenzothiazole part II: zebrafish. Aquat. Toxicol. 173, 204-217.

Strähle, U., et al., 2012. Zebrafish embryos as an alternative to animal experiments—A commentary on the definition of the onset of protected life stages in animal welfare regulations. Rep. Toxicol. 33, 128-132.

Takayama, S., et al., 2008. An F-domain introduced by alternative splicing regulates activity of the zebrafish thyroid hormone receptor α: role of zebrafish TRα F-domain. Gen. Comp. Endocrinol. 155, 176-189.

Thisse, C., et al., 2003. Spatial and temporal expression patterns of selenoprotein genes during embryogenesis in zebrafish. Gene Expr. Patterns 3, 525-532.

Vandesompele, J., et al., 2002. Accurate normalization of real-time quantitative RT-PCR data by geometric averaging of multiple internal control genes. Genome Biol. 3, 1-12.

Vatine, G.D., et al., 2013. Zebrafish as a model for monocarboxyl transporter 8-deficiency. J. Biol. Chem. 288, 169-180.

Villeneuve, D.L., et al., 2007. Transcription of key genes regulating gonadal steroidogenesis in control and ketoconazole- or vinclozolin-exposed fathead minnows. Toxicol. Sci. 98, 395-407.

Villeneuve, D.L., et al., 2014. Investigating alternatives to the fish early-life stage test: a strategy for discovering and annotating adverse outcome pathways for early fish development. Environ. Toxicol. Chem. 33, 158-169.

Wabuke-Bunoti, M.A.N., Firling, C., 1983. The prehatching development of the thyroid gland of the fathead minnow, *Pimephales promelas* (Rafinesque). Gen. Comp. Endocrinol. 49, 320-331.

Walpita, C.N., et al., 2007. The effect of 3,5,3´-triiodothyronine supplementation on zebrafish (*Danio rerio*) embryonic development and expression of iodothyronine deiodinases and thyroid hormone receptors. Gen. Comp. Endocrinol. 152, 206-214.

Walpita, C.N., et al., 2009. Type 2 iodothyronine deiodinase is essential for thyroid hormone-dependent embryonic development and pigmentation in zebrafish. Endocrinol. 150(1), 530-539.

Walpita C.N., Crawford A.D., Darras V.M., 2010. Combined antisense knockdown of type 1 and type 2 iodothyronine deiodinases disrupts embryonic development in zebrafish (*Danio rerio*). Gen. Comp. Endocrinol. 166(1), 134-41.

Wilson, C., 2012. Aspects of larval rearing. ILAR J. 53(2), 169-178.

Wendl, T., et al., 2002. pax2.1 is required for the development of thyroid follicles in zebrafish. Development. 129, 3751-3760.

Wragg, J., Müller, F., 2016. Chapter six – Transcriptional regulation during zygotic genome activation in zebrafish and other anamniote embryos. Advances in Genetics 95, 161-194.

Yu, L.Q., et al., 2010. Exposure to DE-71 alters thyroid hormone levels and gene transcription in the hypothalamic-pituitary-thyroid axis of zebrafish larvae. Aquatic Toxicology 97(3):226-233.

Zoeller, R.T., Tan, S.W., Tyl, R.W., 2007. General background on the hypothalamic-pituitary-thyroid (HPT) axis. Crit. Rev. Toxicol. 37, 11-53.

**Figure Legends**

**Figure 1**. An overview of the teleost hypothalamic-pituitary-thyroid negative feedback axis, based on reviews by Zoeller et al. (2007) and Blanton and Specker (2007), including tissue localization of genes examined in the present ontogeny study. Genes of interest are indicated in red italics. Red crosses indicate negative feedback on the hypothalamus and pituitary mediated by blood plasma thyroid hormone levels.

**Figure 2**. Diagram representing the timeline of select key events during (A) fathead minnow and (B) zebrafish development, from fertilization to juvenile stages. Color bars indicate the developmental phases with gradients representing embryo-larval and larval-juvenile transitions. We chose to extend the period of embryonic development beyond hatching (including the eleutheroembryo), and to mark an embryo-larval transition phase representing the transition to free-feeding among other events (Strähle et al., 2012). The developmental timeline for the fathead minnow is based on reports by Wabuke-Bunoti and Firling (1983), Devlin et al. (1996), and Crane et al. (2004). The timeline for zebrafish is based on Kimmel et al. (1995), Porazzi et al. (2009), Wilson et al. (2012), Villeneuve et al. (2014), Hagenaars et al. (2014), Stinckens et al. (2016), Opitz et al. (2012), Alt et al. (2006), Elsalini et al. (2003), and Chang et al. (2012).

**Figure 3.** Relative quantities of thyrotropin-releasing hormone receptor (*trhr*) and thyroid stimulating hormone receptor (*tshr*) from whole bodies of early-life stage fathead minnows and zebrafish: (A) fathead minnow *trhr2*, (B) fathead minnow *tshr*, (C) zebrafish *trhrb*, and (D) zebrafish *tshr*. The graphs show log2 relative quantities which have been normalized for reference gene expression and expressed relative to the time point with the lowest expression. Data points represent mean (±SD) of n = 6-8 replicate pools for fathead minnow and 4 replicate pools for zebrafish at each time point (dpf = days post-fertilization). In the zebrafish graphs, the first (1.5 hpf) time point was omitted because the transcript could not be detected. The red line indicates the loess fit of the gene target, and the surrounding dashed blue line indicates the 95% confidence interval around the loess fit. The green and purple highlighted regions represent the 95% and 99% confidence intervals, respectively, of each critical point (minimum or maximum) of mRNA expression. An asterisk (*) indicates the data point for unfertilized eggs from the maternal transfer test. The most relevant developmental events for interpretation of the profiles

are indicated using full lines. Tf: appearance of the first thyroid follicles, H: hatching, Psb: posterior swim bladder chamber inflation, Asb: anterior swim bladder chamber inflation. The approximate timeline for the different developmental stages is displayed in the green/blue color bar.

**Figure 4.** Relative quantities of sodium-iodide symporter (*nis*) and thyroid peroxidase (*tpo*) from whole bodies of early-life stage fathead minnows and zebrafish: (A) fathead minnow *nis*, (B) fathead minnow *tpo*, (C) zebrafish *nis*, and (D) zebrafish *tpo*. The graphs show log2 relative quantities which have been normalized for reference gene expression and expressed relative to the time point with the lowest expression. Data points represent mean (±SD) of n = 6-8 replicate pools for fathead minnow and 4 replicate pools for zebrafish at each time point (dpf = days post-fertilization). The red line indicates the loess fit of the gene target, and the surrounding dashed blue line indicates the 95% confidence interval around the loess fit. The green and purple highlighted regions represent the 95% and 99% confidence intervals, respectively, of each critical point (minimum and maximum) of mRNA expression. An asterisk (*) indicates the data point for unfertilized eggs from the maternal transfer test. The most relevant developmental events for interpretation of the profiles are indicated using full lines. Tf: appearance of the first thyroid follicles, H: hatching, Psb: posterior swim bladder chamber inflation, Asb: anterior swim bladder chamber inflation. The approximate timeline for the different developmental stages is displayed in the green/blue color bar.

**Figure 5.** Relative quantities of thyroglobulin (*tg*) and transthyretin (*ttr*) from whole bodies of early-life stage fathead minnows and zebrafish: (A) fathead minnow *tg*, (B) fathead minnow *ttr*, (C) zebrafish *tg*, and (D) zebrafish *ttr*. The graphs show log2 relative quantities which have been normalized for reference gene expression and expressed relative to the time point with the lowest expression. Data points represent mean (±SD) of n = 6-8 replicate pools for fathead minnow and 4 replicate pools for zebrafish at each time point (dpf = days post-fertilization). The red line indicates the loess fit of the gene target, and the surrounding dashed blue line indicates the 95% confidence interval around the loess fit. The green and purple highlighted regions represent the 95% and 99% confidence intervals, respectively, of each critical point (minimum and maximum) of mRNA expression. An asterisk (*) indicates the data point for unfertilized eggs from the

maternal transfer test. The most relevant developmental events for interpretation of the profiles are indicated using full lines. Tf: appearance of the first thyroid follicles, H: hatching, Psb: posterior swim bladder chamber inflation, Asb: anterior swim bladder chamber inflation. The approximate timeline for the different developmental stages is displayed in the green/blue color bar.

**Figure 6.** Relative quantities of deiodinases 1, 2, and 3 (*dio1-3)* from whole bodies of early-life stage fathead minnows and zebrafish: (A) fathead minnow *dio1*, (B) fathead minnow *dio2*, (C) zebrafish *dio1*, (D) zebrafish *dio2*, (E) zebrafish *dio3a,* and (F) zebrafish *dio3b*. The graphs show log2 relative quantities which have been normalized for reference gene expression and expressed relative to the time point with the lowest expression. Data points represent mean (±SD) of n = 6-8 replicate pools for fathead minnow and 4 replicate pools for zebrafish at each time point (dpf = days post-fertilization). The red line indicates the loess fit of the gene target, and the surrounding dashed blue line indicates the 95% confidence interval around the loess fit. The green and purple highlighted regions represent the 95% and 99% confidence intervals, respectively, of each critical point (minimum and maximum) of mRNA expression. An asterisk (*) indicates the data point for unfertilized eggs from the maternal transfer test. The most relevant developmental events for interpretation of the profiles are indicated using full lines. Tf: appearance of the first thyroid follicles, H: hatching, Psb: posterior swim bladder chamber inflation, Asb: anterior swim bladder chamber inflation. The approximate timeline for the different developmental stages is displayed in the green/blue color bar.

**Figure 7.** Relative quantities of thyroid hormone receptors α and β *(thrα* and *β*) from whole bodies of early-life stage fathead minnows and zebrafish: (A) fathead minnow *thrα*, (B) fathead minnow *thrβ*, (C) zebrafish *thrα*, and (D) zebrafish *thrβ*. The graphs show log2 relative quantities which have been normalized for reference gene expression and expressed relative to the time point with the lowest expression. Data points represent mean (±SD) of n = 6-8 replicate pools for fathead minnow and 4 replicate pools for zebrafish at each time point (dpf = days post-fertilization). The red line indicates the loess fit of the gene target, and the surrounding dashed blue line indicates the 95% confidence interval around the loess fit. The green and purple highlighted regions represent the 95% and 99% confidence intervals, respectively, of each

critical point (minimum and maximum) of mRNA expression. An asterisk (*) indicates the data point for unfertilized eggs from the maternal transfer test. The most relevant developmental events for interpretation of the profiles are indicated using full lines. Tf: appearance of the first thyroid follicles, H: hatching, Psb: posterior swim bladder chamber inflation, Asb: anterior swim bladder chamber inflation. The approximate timeline for the different developmental stages is displayed in the green/blue color bar.

**Figure 8**. Biplot resulting from a principal component analysis of all transcript levels at 21 similar time points (days post-fertilization) from both species. The positions of the time points are shown as a function of the first and second principal component. The time points were connected to show species-specific paths allowing for inter-species comparison. The first and second PC accounted for 64 and 11% of the variation in the dataset respectively.

**Abbreviations:**

AOP = adverse outcome pathway

bactin = beta actin

dio = deiodinase

dpf = days post-fertilization

dph = days post-hatch

EDC = endocrine disrupting chemical

hpf = hours post-fertilization

HPT = hypothalamic-pituitary-thyroid

LSW = Lake Superior water

nis = sodium-iodide symporter

qPCR = quantitative polymerase chain reaction

qRT-PCR = quantitative reverse transcriptase polymerase chain reaction

rp18 = ribosomal protein 18

rpnl = Ribophorin 1

tg = thyroglobulin

TH = thyroid hormone

thr = thyroid hormone receptor

tpo = thyroid peroxidase

trh = thyrotropin-releasing hormone

trhr = thyrotropin releasing hormone receptor

tsh = thyroid stimulating hormone

tshr = thyroid stimulating hormone receptor

ttr = transthyretin

T3 = 3,5,3'-triiodothyronine

T4 = L-thyroxine

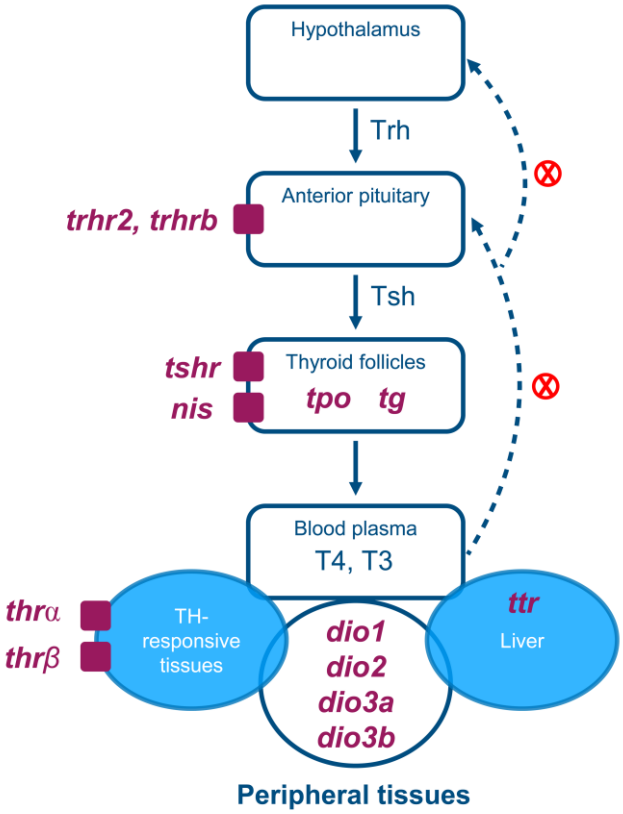

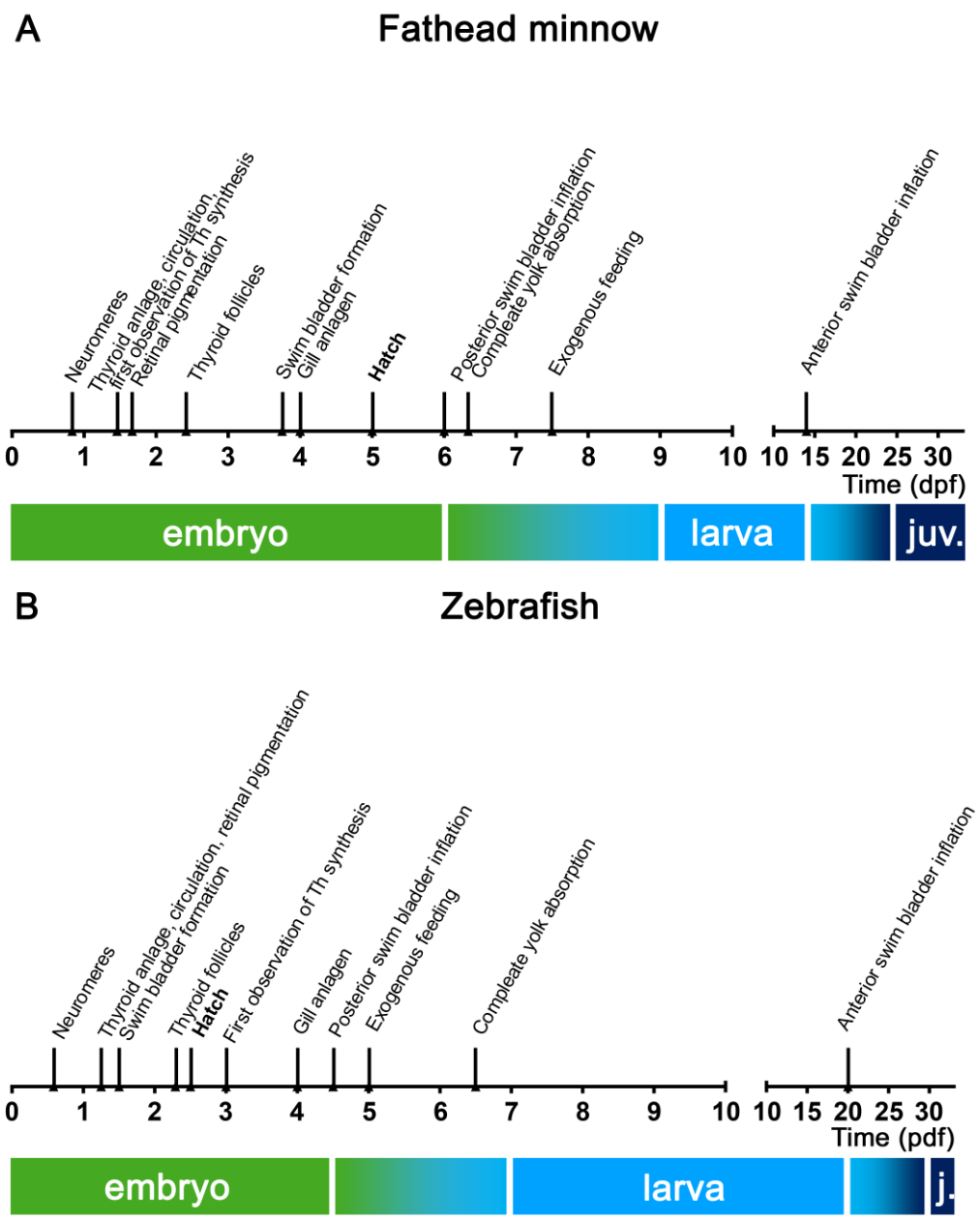

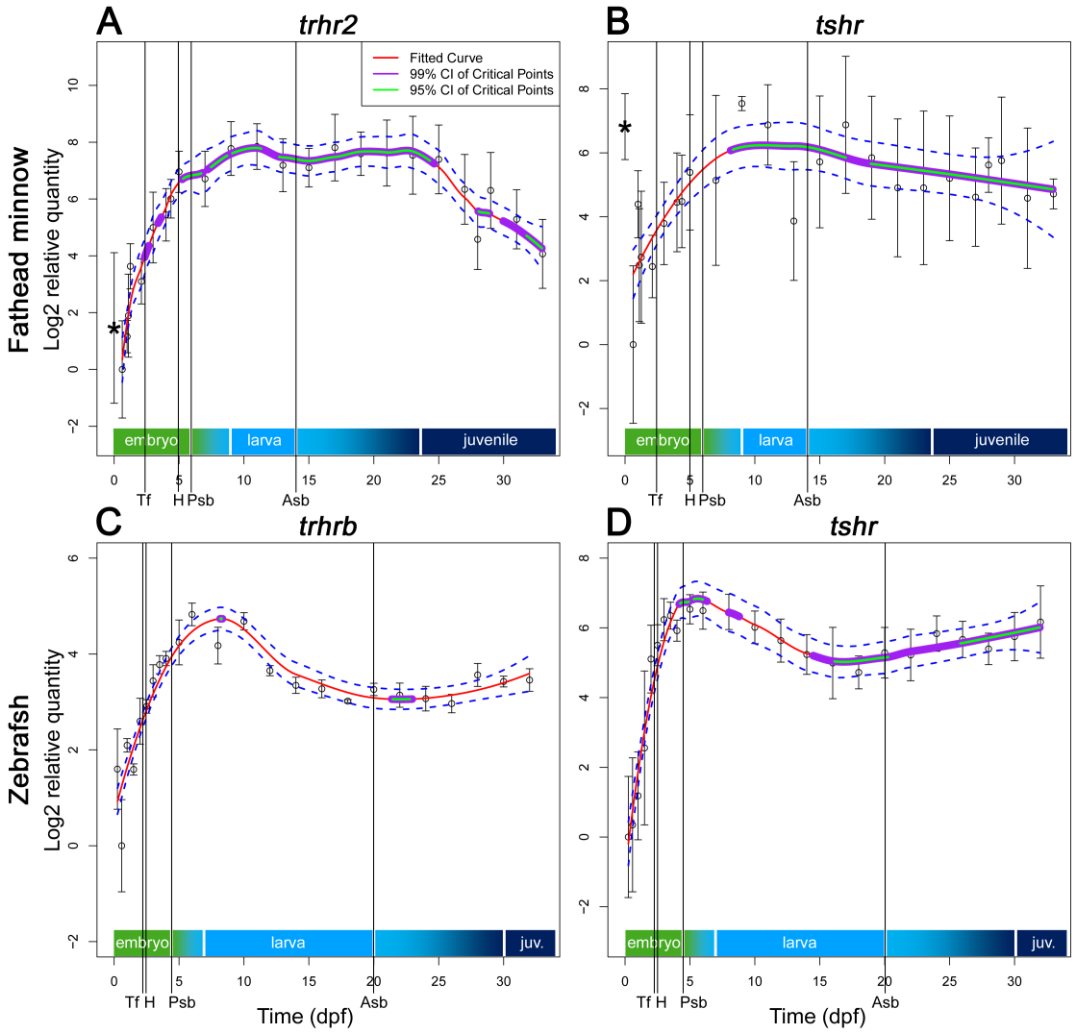

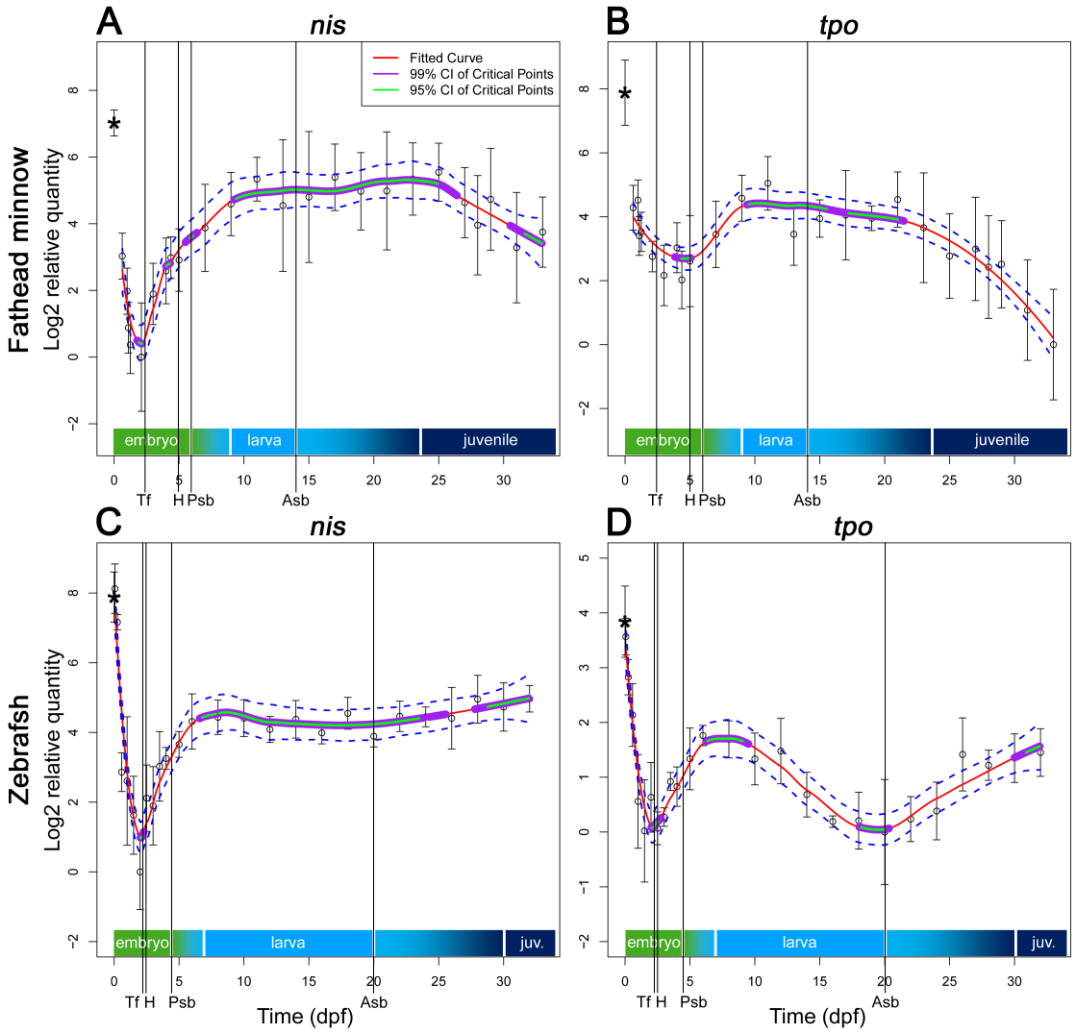

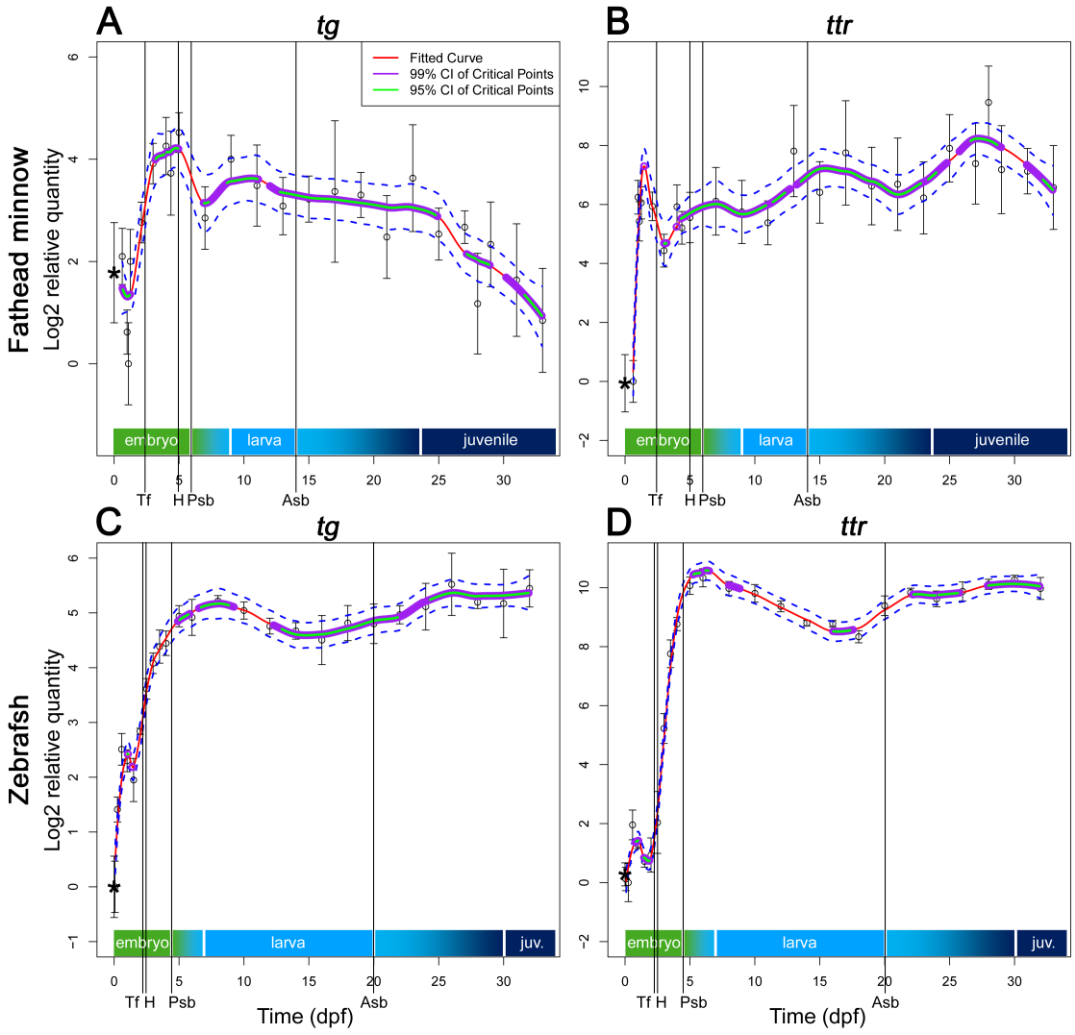

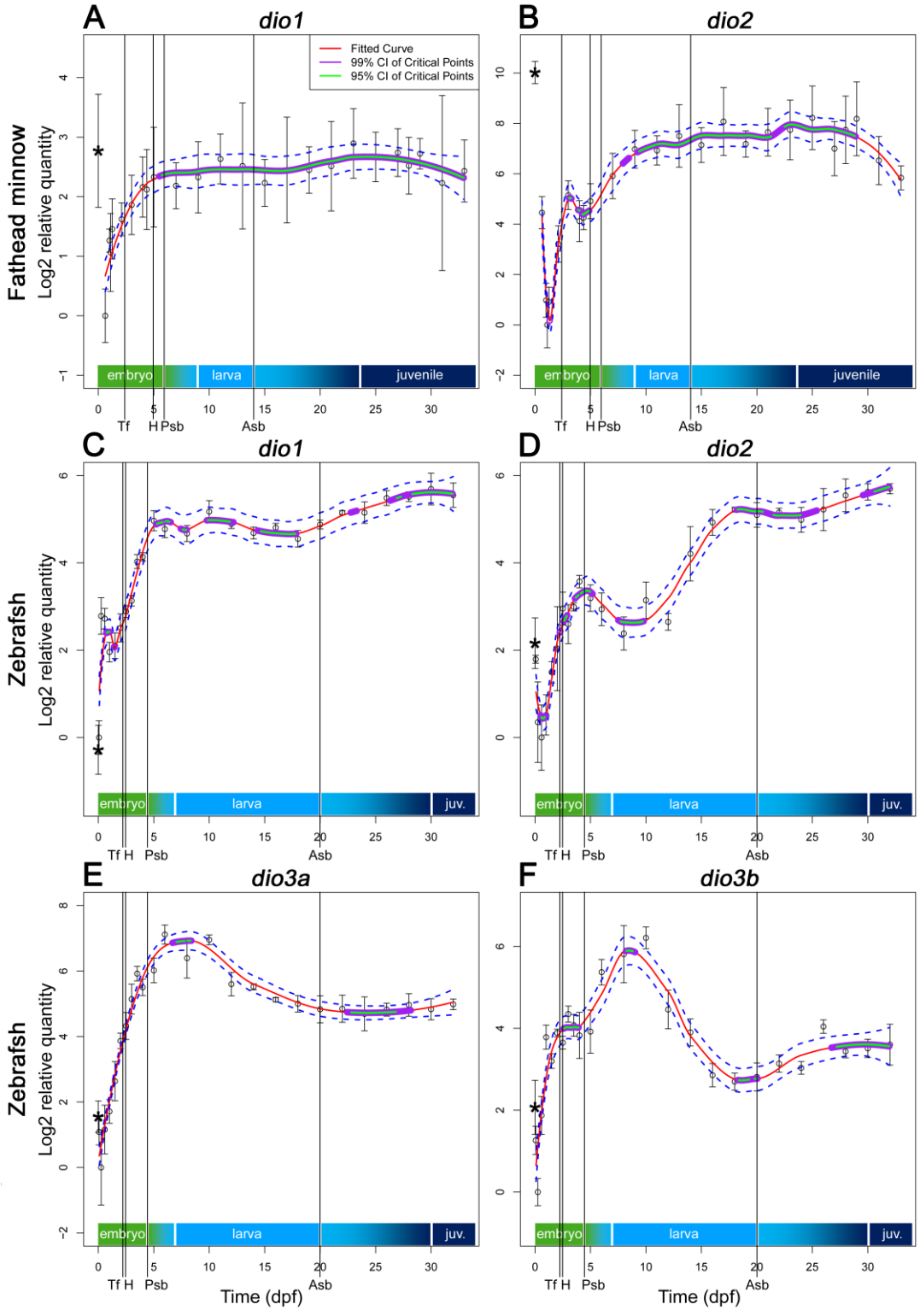

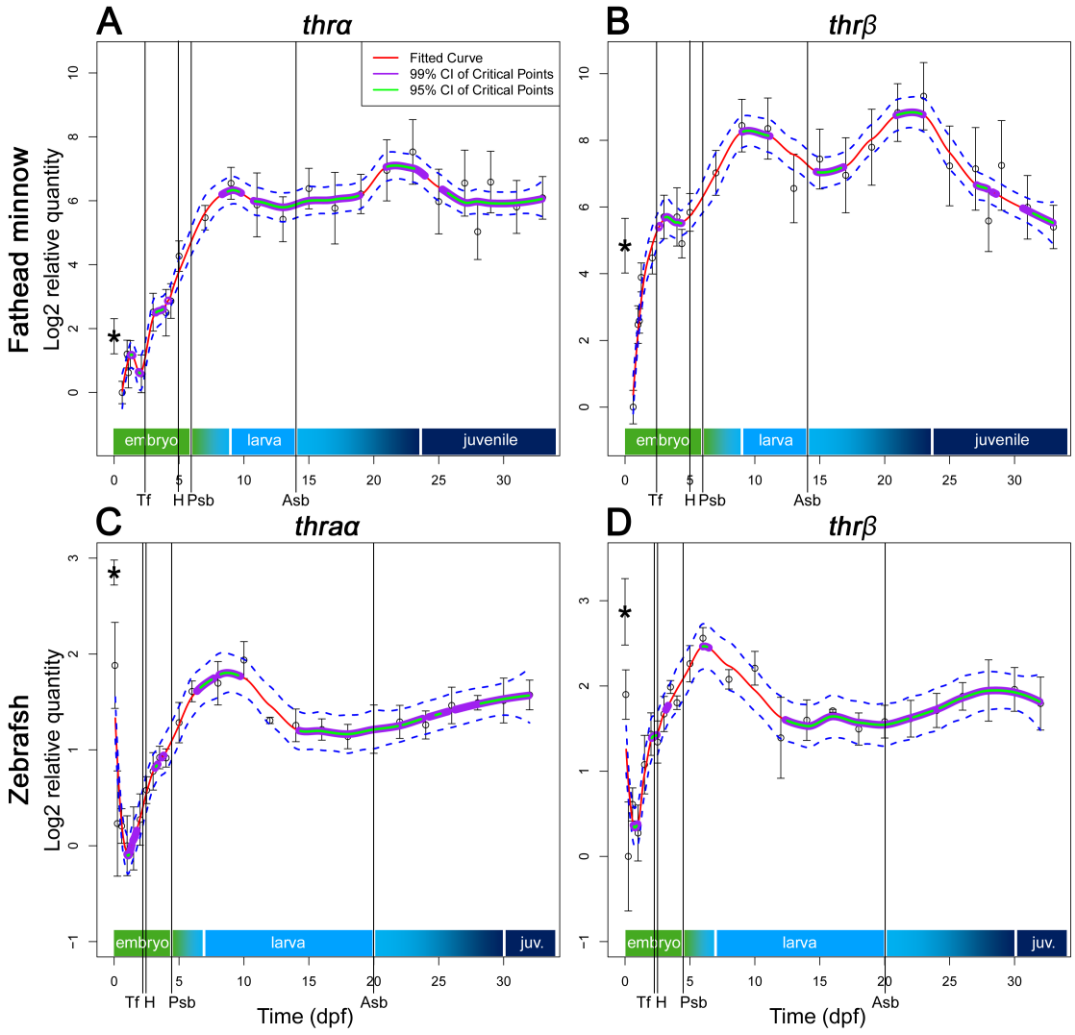

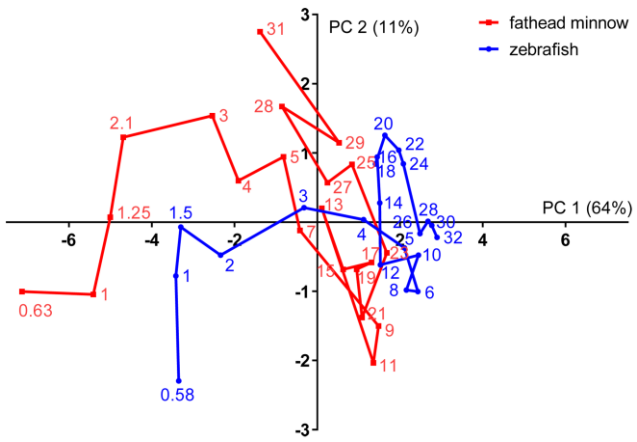

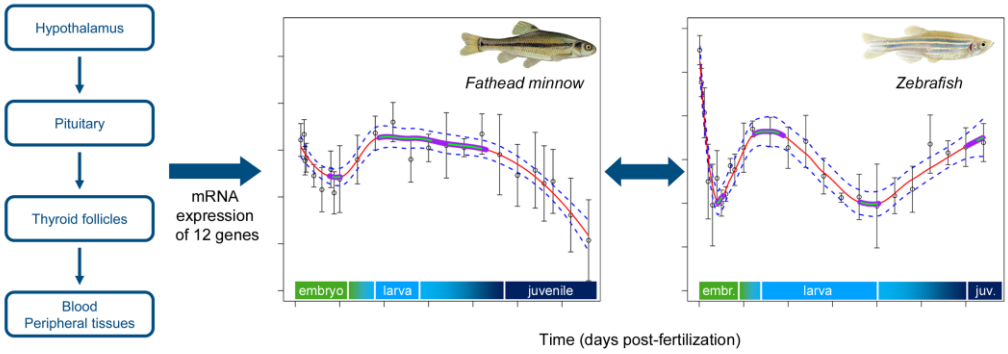

**Highlights**

- Control fish were sampled at 25 time points covering embryo-larval development
- Transcript levels of 12 thyroid-related genes were profiled
- Maternal transfer of almost all transcripts was confirmed in unfertilized eggs
- Increasing transcript levels up to larval period suggest active HPT-axis in larvae
- Inter-species comparison of profiles showed an overall high similarity